International Journal of Microwave and Wireless Technologies

cambridge.org/mrf

Meta-heuristic optimization algorithms for synthesis of reconfigurable hexagonal array antenna in two principle vertical planes

Bitan Misra and Gautam Kumar Mahanti

Department of Electronics and Communication Engineering, National Institute of Technology, Durgapur, West Bengal, India

Research Paper

Cite this article: Misra B, Mahanti GK (2022). Meta-heuristic optimization algorithms for synthesis of reconfigurable hexagonal array antenna in two principle vertical planes. *International Journal of Microwave and Wireless Technologies* **14**, 158–165. https://doi.org/10.1017/S1759078721000337

Received: 23 November 2020
Revised: 16 February 2021
Accepted: 17 February 2021
First published online: 26 April 2021

Key words:
Meta-heuristic algorithms; hexagonal array antenna; pencil beam; flat-top beam

Author for correspondence:
Bitan Misra,
E-mail: misra.bitan2013@gmail.com

Abstract

This study illustrates the dynamical reconfiguration of a concentric hexagonal antenna array radiation to generate a pencil beam and flat-top beam simultaneously by electronic control in two principle vertical planes under consideration. Both the beams share a common normalized optimal current excitation amplitude distribution while the optimal sets of phase excitation coefficients are varied radically across the hexagons to generate a flat-top beam. The proposed approach is able to solve the underlying multi-objective problem and flexible enough to the efficient implementation of additional design constraints in the considered φ-planes. In this paper, a set of simulation-based examples are presented in an integrated way. The outcomes validate the effectiveness of the stated optimization using meta-heuristic optimization algorithms (teaching–learning-based optimization, symbiotic organism search, multi-verse optimization) to reach the solution globally and prove actual relevance to the concerned applications.

Introduction

In many practical applications such as high-performance radar systems, Wireless Local Area Network (WLAN), satellite communications, spacecraft applications, mobile communications an antenna array should be able to reconfigure different patterns to perform various tasks. The advantage of such an array design is that it reduces the design cost and save space for the electronic payload still ensuring the generation of different beam shapes in the radiation pattern [1]. Among various types of adopted radiating structures, controlling the excitation phase of the antennas is found to be more efficient because of the flexibility of the reconfiguration and the ease of ability to act on the design of the feeding network using power divider and phase shift. Therefore, in practice, phase-only reconfigurable array antennas are preferred over the amplitude excitation because of their inessentiality of additional hardware [2–10].

The synthesis approach is necessary to fulfil multiple requirements and also it needs to incorporate the design constraints. The intersection method [2] or succesive projection approach method [3] are simple, but not fit enough to deal with the non-linear design problems, sensitive to the initial values and obtain local solutions only. Over the year, different evolutionary algorithms have proven to be more effective for such synthesis problems and globally explore the solution in the search space. Particle swarm optimization [4, 5], genetic algorithm [6, 7], biogeography-based optimization [8], invasive weed optimization [9], symbiotic organism search [10] methods have shown their flexibility to reach the design goal. With the advancement in technology, the speed of the processors has increased rapidly, resulting in lower time consumption to reach the optimal solutions and making these methods more popular with the researchers.

In this paper, meta-heuristic algorithms are applied for the optimization of the problem at hand and to deal with constraints to make the design suitable for practical realization. The proposed approach combines multiple objectives such as low sidelobe level and ripple into a single cost function that needs to be minimized. Moreover, this approach can deal with the constraint of the mutual coupling effect. Teaching–learning-based optimization (TLBO), symbiotic organism search (SOS), and multi verse optimization (MVO) methods are chosen because of their proven effectiveness reported in various kinds of literature [10–13]. The proposed design approach is suitable for effective application in optimal wireless monitoring technologies, biomedical, and health monitoring systems [14]. The detailed working principles of TLBO, SOS, and MVO can be found in [15–17], respectively.

Two simulation-based examples for a concentric hexagonal array [18–20] antenna structures are performed to retrieve the pencil and flat-top beams by exploiting a fixed number of elements in the array structure. A typical excitation current ranging between 0 and 1 is fed to the array elements for generating both the beams. The excitation phase is varied

© The Author(s), 2021. Published by Cambridge University Press in association with the European Microwave Association

CAMBRIDGE UNIVERSITY PRESS

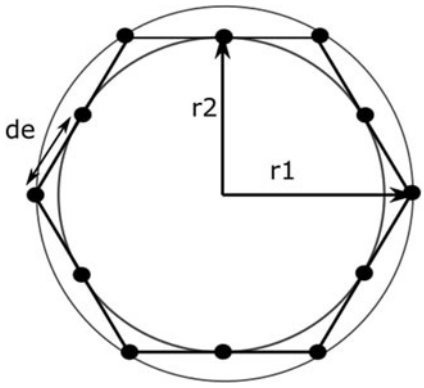


Fig. 1. Hexagonal antenna array.

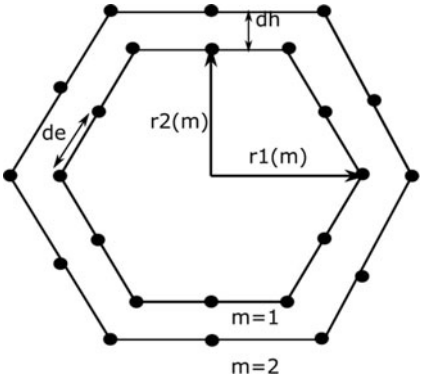


Fig. 2. A concentric hexagonal antenna array.

radically between −180° and 180° for the flat-top beam generation, whereas the pencil beam is employed with zero excitation current. The analysis of the results at two principle φ-planes will assess the feasibility and benefits of the proposed approach. The ability of the proposed hexagonal array to generate reconfigurable beam patterns with optimal common current excitation at different azimuth angles makes this paper unique and suitable for high-performance radar and satellite communication.

From the literature review, it is found that Mahmoud *et al.* [20] and Bera *et al.* [21] have designed an 18-element hexagonal array antenna, but the details of the equations to calculate the radial distance and the angular positions are not provided in this paper. Here we have presented the design equations along with the simulated structures to generate a pencil beam and a flat-top beam by varying phase only in the principle vertical planes.

The rest of the paper is presented as follows. "Problem statement" is allocated to the construction of the problem and details discussion of the proposed design. "Simulation-based performance assessment" is devoted to some simulation-based examples and analysis of the outcomes. "Conclusion" illustrates the paper with conclusions and followed up by some possible future extension of the proposition.

Problem statement

The geometry of a hexagonal array antenna can be developed using two concentric ring arrays of different radius. Figure 1 represents a hexagonal array of 2*N* isotropic elements placed in the *x*–*y* plane. The general array factor expression of a hexagonal array antenna can be given as:

$$AF(\theta, \varphi) = \sum_{n=1}^{N} [\, A_n \, e^{jk\, r_1 \sin\theta(\cos\phi_{1n}\cos\varphi + \sin\phi_{1n}\sin\varphi)} + B_n \, e^{jk\, r_2 \sin\theta(\cos\phi_{2n}\cos\varphi + \sin\phi_{2n}\sin\varphi)} \,], \quad (1)$$

where A_n represents the excitation current amplitude of the *n*th element located at the vertices of the hexagonal array and B_n

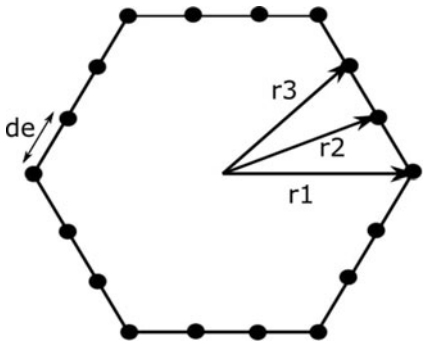


Fig. 3. 18-Element uniform hexagonal array antenna.

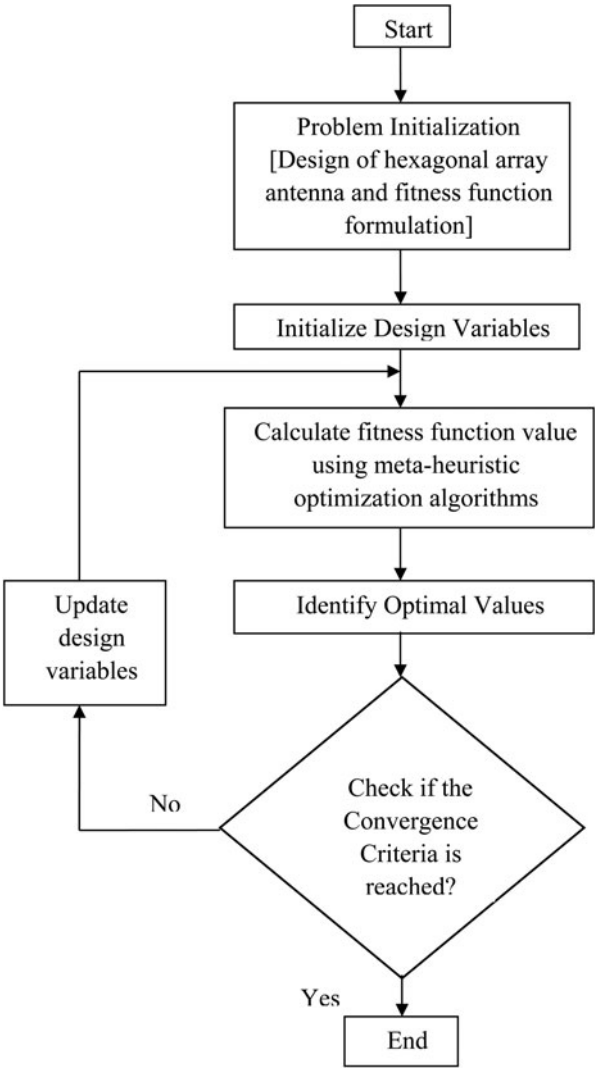


Fig. 4. Flowchart of the synthesis process.

https://doi.org/10.1017/S1759078721000337 Published online by Cambridge University Press

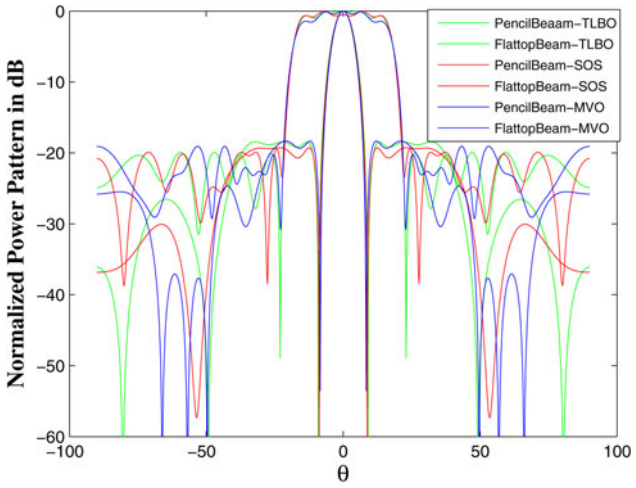


Fig. 5. Normalized power pattern in $\varphi = 0^{o}$ plane for Example 1.

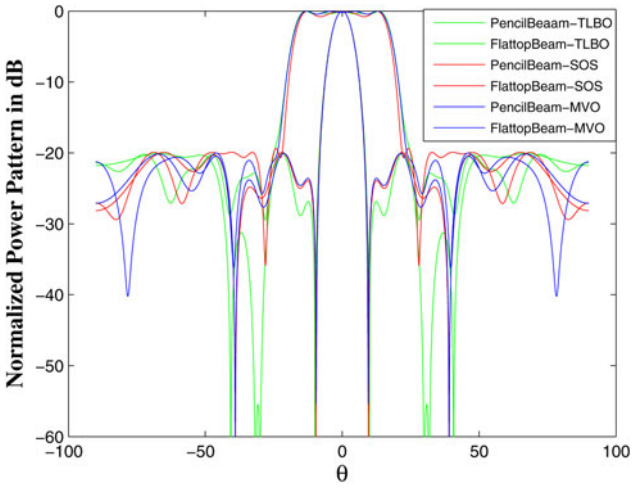


Fig. 6. Normalized power pattern in $\varphi = 90^{o}$ plane for Example 1.

represents the current excitation amplitude of the nth element located in the middle of each arm of the hexagonal array antenna. Here θ is the elevation angle ($\theta \in [-\pi/2, \pi/2]$) and φ is the azimuth angle ($\varphi \in [0, 2\pi]$).

The circumferential curve of the vertices of the hexagonal array is contrived by a circular array of radius r_1 and consists of N number of isotropic array elements. The circumferential curve consists of the array elements present in the middle of each arm of the hexagon can be depicted using a circular array of radius r_2, comprising N isotropic elements. These r_1 and r_2 are related as follows:

$$\begin{aligned} r_2 &= r_1 \times \cos(\pi/N), \\ r_1 &= d_e \times \sin(\pi/N), \end{aligned} \tag{2}$$

where d_e is the inter-element spacing. The angular location of the antennas located at the vertices of the hexagonal array antenna is given as follows:

$$\phi_{1n} = \frac{2\pi(N-1)}{N}. \tag{3}$$

The angular location of the antennas present at the middle of each arm of the hexagonal array is given as follows:

$$\phi_{2n} = \phi_{1n} + \frac{\pi}{N}. \tag{4}$$

In this paper, we have considered a concentric array of hexagonal antennas to reconfigure the beam shaped in the radiation pattern. The geometry of a concentric hexagonal array antenna is shown in Fig. 2. The array factor for M concentric hexagonal array antennas is expressed as

$$AF(\theta, \varphi) = \sum_{m=1}^{M}\sum_{n=1}^{N} \left[A_m e^{jk r_{1m} \sin\theta(\cos\phi_{1n}\cos\varphi + \sin\phi_{1n}\sin\varphi)} + B_m e^{jk r_{2m} \sin\theta(\cos\phi_{2n}\cos\varphi + \sin\phi_{2n}\sin\varphi)} \right]. \tag{5}$$

Each hexagon in the array has a $2N$ number of isotropic antennas. A_m and B_m are the amplitudes of the excitation current of the elements present at the vertices and the middle of each arm of the mth hexagon, respectively,

$$\begin{aligned} r_{1m} &= r + (m-1)\, d_h, \\ r_{2m} &= r_{1m} \times \cos(\pi/N), \end{aligned} \tag{6}$$

where r represents the radius of the outer circle of the innermost hexagon of a hexagonal antenna array.

A hexagonal array antenna with $3N$ isotropic antennas is shown in Fig. 3. There are one element in each vertex and two elements in each arm. The array factor can be expressed as

$$AF(\theta, \varphi) = \sum_{m=1}^{M}\sum_{n=1}^{N} \left[A_n e^{jk r_1 \sin\theta(\cos\phi_{1n}\cos\varphi + \sin\phi_{1n}\sin\varphi)} + B_n e^{jk r_2 \sin\theta(\cos\phi_{2n}\cos\varphi + \sin\phi_{2n}\sin\varphi)} + C_n e^{jk r_3 \sin\theta(\cos\phi_{3n}\cos\varphi + \sin\phi_{3n}\sin\varphi)} \right]. \tag{5}$$

where C_n is the amplitude of the element having the radial distance r_3. r_2 and r_3 represent the radial distance of the antennas

Table 1. Desired and obtained simulation values for Example 1.

Case	Design variables	Desired value	TLBO obtained value	SOS obtained value	MVO obtained value
Case 1 ($\varphi = 0^{o}$)	SLL (pencil beam)	−20 dB	−18.44	−19.27	−18.33
	SLL (flat-top beam)	−20 dB	−19.91	−19.91	−19.07
	Ripple	0.5	1.01	0.88	1.63
Case 2 ($\varphi = 90^{o}$)	SLL (pencil beam)	−20 dB	−20.01	−19.92	−20.02
	SLL (flat-top beam)	−20 dB	−20.18	−19.91	−20.45
	Ripple	0.5	0.45	0.79	0.48

https://doi.org/10.1017/S1759078721000337 Published online by Cambridge University Press

https://doi.org/10.1017/S1759078721000337 Published online by Cambridge University Press

Table 2. Optimal set of radial phase excitation (in degrees) for flat-top beam and common normalized amplitude distribution for both the beams in Example 1.

				Position of the hexagonal array							
Case	Algorithms	Position of the elements	Amplitude and phase excitation	1	2	3	4	5	6	7	8
Case 1	TLBO	Vertices	Phase excitation	−87.68	28.23	65.48	55.34	42.03	90.92	86.38	146.21
			Amplitude excitation	0.42	0.94	0.98	0.66	0.40	0.27	0.37	0.20
		Arm	Phase excitation	−87.26	−79.37	43.60	−59.33	−20.26	96.86	150.56	−149.46
			Amplitude excitation	0.75	0.34	0.25	0.45	0.33	0.34	0.29	0.35
	SOS	Vertices	Phase excitation	−108.32	3.81	11.55	−6.35	17.81	8.76	146.94	9.15
			Amplitude excitation	0.76	0.72	0.87	0.67	0.42	0.28	0.58	0.33
		Arm	Phase excitation	−127.34	153.10	−48.81	−102.50	−6.19	33.64	147.31	4.40
			Amplitude excitation	0.73	0.37	0.37	0.33	0.40	0.15	0.77	0.18
	MVO	Vertices	Phase excitation	−5.93	131.85	142.88	158.28	171.07	174.72	4.03	179.72
			Amplitude excitation	0.17	0.97	0.86	0.82	0.64	0.72	0.23	0.79
		Arm	Phase excitation	2.61	4.42	42.44	107.19	18.85	158.36	−14.04	−133.35
			Amplitude excitation	0.93	0.24	0.74	0.09	0.22	0.40	0.61	0.37
Case 2	TLBO	Vertices	Phase excitation	−56.22	−15.07	−82.86	68.00	−107.92	120.22	142.90	−167.82
			Amplitude excitation	0.47	0.45	0.72	0.30	0.29	0.40	0.58	0.23
		Arm	Phase excitation	−142.00	−74.54	−27.41	29.22	59.52	45.23	−40.22	76.93
			Amplitude excitation	0.93	0.57	0.46	0.73	0.44	0.42	0.19	0.25
	SOS	Vertices	Phase excitation	−36.31	50.40	−92.77	−18.71	−128.42	−145.24	−145.01	−129.99
			Amplitude excitation	0.44	0.52	0.55	0.40	0.43	0.39	0.13	0.37
		Arm	Phase excitation	−120.30	−74.88	43.04	−10.90	53.59	57.34	121.12	79.20
			Amplitude excitation	0.99	0.66	0.52	0.67	0.48	0.50	0.37	0.33
	MVO	Vertices	Phase excitation	23.80	−64.01	9.33	37.84	138.91	126.45	98.20	163.21
			Amplitude excitation	0.36	0.35	0.27	0.30	0.48	0.17	0.23	0.36
		Arm	Phase excitation	114.45	31.12	61.19	−83.41	−46.78	−93.55	−126.72	−43.60
			Amplitude excitation	0.64	0.46	0.61	0.57	0.31	0.43	0.18	0.25

Table 3. Desired and obtained simulation values for Example 2.

Case	Design variables	Desired value	TLBO obtained value	SOS obtained value	MVO obtained value
Case 1 ($\varphi = 0^o$)	SLL (pencil beam)	−20 dB	−20.00	−20.37	−20.03
	SLL (flat-top beam)	−20 dB	−20.15	−20.07	−20.11
	Ripple	0.5	0.49	0.47	0.53
Case 2 ($\varphi = 90^o$)	SLL (pencil beam)	−20 dB	−20.01	−20.01	−20.65
	SLL (flat-top beam)	−20 dB	−20.01	−20.09	−20.60
	Ripple	0.5	0.51	0.49	0.36

present in each arm and r_1 represents the radial distance of the elements present at the vertices of the hexagon, as shown in Fig. 3.

$$\begin{aligned} r_3 &= \sqrt{3} \times (d_e / \sin(\phi_{3n})), \\ r_2 &= \sqrt{3}/2 \times (d_e / \sin(\phi_{2n})), \\ r_1 &= d_e \times \sin(\pi/N), \end{aligned} \tag{8}$$

where d_e is the inter-element spacing and ϕ_{2n}, ϕ_{3n} are the angular positions of the elements present in each arm, calculated from the positive x-axis, as shown in Fig. 3. These values can be obtained using the equations below:

$$\begin{aligned} \phi_{3n} &= \phi_{1n} + \tan^{-1}(\sqrt{3}/((r/) - 1)), \\ \phi_{2n} &= \phi_{1n} + \tan^{-1}(\sqrt{3}/((2 \times r/ d_e) - 1)), \\ \phi_{1n} &= 2\pi(n-1)/N. \end{aligned} \tag{9}$$

The normalized far-field radiation pattern in dB can be expressed as

$$AF_{norm} = 20 \log_{10}\left[\frac{|AF(\theta, \varphi)|}{|AF(\theta, \varphi)|_{\max}}\right]. \tag{10}$$

To generate reconfigurable beam patterns, we need to achieve the best common excitation current amplitude distribution across the radius of the hexagons using meta-heuristic algorithms. The current amplitudes for all the elements, A_m and B_m are kept between 0 and 1 and varied across the radius of the hexagon of the hexagonal array antenna. Moreover, a smooth amplitude distribution with lower variation is targeted to achieve more control over the mutual coupling effect and to increase the efficiency. For the pencil beam generation, the phase of the excitation current is kept at 0. For the generation of a flat-top beam, the phase of the excitation current is varied radically across the hexagonal array antenna. The complex excitation of the elements present at the vertices and the middle of each side of the mth hexagon is represented as $A_m e^{j\,Phase_m}$ and $B_m e^{j\,Phase_m}$, respectively, where $Phase_m \in [-2\pi, 2\pi]$.

The design objective is modeled as a minimization problem. The goal is to reduce the SLL value for the pencil beam and flat-top beam. Also, the Reduction of the ripples in the main beam of the flat top radiation pattern is another objective. The cost function (CF) to be minimized can be expressed as

$$\mathrm{CF} = C1 \cdot \mathrm{CF1} + C2 \cdot \mathrm{CF2} + C3 \cdot \mathrm{CF3}, \tag{11}$$

where CF1 and CF2 are the cost functions that minimize the side-lobe levels for pencil beam and flat-top beam, respectively, and are given as follows:

$$\begin{aligned} \mathrm{CF1} &= (\mathrm{SLLd} = \mathrm{SLLc})^2 \text{subject to } \theta \\ &\in \{[-90^\circ, -|FN|\&|FN|, 90^\circ]\}, \end{aligned} \tag{12}$$

$$\begin{aligned} \mathrm{CF2} &= (\mathrm{SLLd} = \mathrm{SLLc})^2 \text{subject to } \theta \\ &\in \{[-90^\circ, |FNL|\&|FNU|, 90^\circ]\}, \end{aligned} \tag{13}$$

$$\mathrm{CF3} = (\mathrm{Rd} = \mathrm{Rc})^2 \text{subject to } \theta \in \{[|FNL|, |FNU|]\}, \tag{14}$$

where SLLd and SLLc represent the desired and computed side-lobe levels, respectively. Again, Rd and Rc are the expected and calculated values of ripples in the main beam of the flat-top radiation, respectively. FN represents the first null value in degree for the pencil beam and FNL and FNU are the lower and upper first null values for flat-top beam, respectively. $C1$, $C2$, and $C3$ are the weighing components that decide the correlative significance of each term. The values of these coefficients are set as $C1 = C2 = C3 = 1$. It is worth noting that different priorities can be assigned by varying the values of the weighing factors to give more stress on optimizing particular radiation pattern characteristics to suit the needs of the design problem. The proposed design is optimized to achieve a reconfigurable radiation pattern at different φ-planes. The proposed synthesis method to design a phase-only reconfigurable hexagonal array antenna is represented with the help of a flowchart (Fig. 4).

Simulation-based performance assessment

The method proposed in the paper is applied to several significant examples to analyze the performance of a reconfigurable array structure. The meta-heuristic optimization algorithms have an initial population size of 30 and the maximum iteration number is 500. The detailed working principles of TLBO, SOS, and MVO can be found in [14–16], respectively.

In Example 1, we have considered the eight-concentric hexagonal array of $3N$ ($N = 6$) isotropic antennas in each hexagon. The spacing between the elements of the first hexagonal array antenna is kept fixed at $d_e = 0.5\lambda$ and the inter-ring spacing is $d_h = 0.5\lambda$. Four different cases are considered for other φ-planes. In Case 1, the optimization is carried out at the 0^o φ-plane and in Case 2, the optimization is performed at the 90^o φ-plane. The normalized synthesized power pattern together using all three algorithms is presented in Figs 5 and 6, for Case 1 and Case 2, respectively. The expected and calculated values of all

https://doi.org/10.1017/S1759078721000337 Published online by Cambridge University Press

https://doi.org/10.1017/S1759078721000337 Published online by Cambridge University Press

Table 4. Optimal set of radial phase excitation (in degrees) for flat-top beam and common normalized amplitude distribution for both the beams in Example 2.

				Number of hexagons							
Case	Algorithms	Position of the elements	Phase and amplitude excitation	1	2	3	4	5	6	7	8
Case 1	TLBO	Vertices	Phase excitation	−103.71	−49.96	44.20	7.53	115.92	17.44	120.35	54.52
			Amplitude excitation	0.51	0.64	0.70	0.27	0.58	0.64	0.19	0.32
		Arm	Phase excitation	−129.76	−100.72	−75.74	−72.52	−112.76	26.69	−50.56	−149.72
			Amplitude excitation	0.68	0.24	0.35	0.29	0.16	0.30	0.23	0.34
	SOS	Vertices	Phase excitation	−111.04	−13.18	59.72	56.90	72.27	−3.56	110.57	63.58
			Amplitude excitation	0.63	0.71	0.04	0.56	0.60	0.18	0.34	0.38
		Arm	Phase excitation	−111.06	−81.60	−121.82	−24.72	3.32	−84.48	111.10	−109.63
			Amplitude excitation	0.59	0.28	0.50	0.43	0.20	0.43	0.02	0.25
	MVO	Vertices	Phase excitation	−70.66	11.48	81.10	93.76	160.93	61.81	179.90	114.79
			Amplitude excitation	0.95	0.53	0.36	0.59	0.52	0.47	0.31	0.28
		Arm	Phase excitation	−60.15	−58.08	−58.56	13.12	7.64	−32.75	62.02	−87.72
			Amplitude excitation	0.36	0.40	0.44	0.39	0.06	0.39	0.08	0.48
Case 2	TLBO	Vertices	Phase excitation	148.76	52.83	118.74	6.76	−141.82	99.30	94.48	98.28
			Amplitude excitation	0.18	0.49	0.21	0.36	0.19	0.07	0.20	0.27
		Arm	Phase excitation	79.18	63.46	−11.53	−158.15	−76.64	−3.32	−125.46	−86.67
			Amplitude excitation	0.97	0.29	0.53	0.24	0.32	0.16	0.32	0.29
	SOS	Vertices	Phase excitation	−11.46	−2.84	−25.92	−90.97	97.69	−62.47	36.30	31.78
			Amplitude excitation	0.69	0.37	0.48	0.51	0.23	0.31	0.50	0.29
		Arm	Phase excitation	8.14	−56.55	−9.53	152.54	−112.18	114.82	−151.42	179.46
			Amplitude excitation	0.97	0.74	0.20	0.60	0.78	0.51	0.49	0.39
	MVO	Vertices	Phase excitation	−19.73	−52.20	−37.13	−168.64	−14.73	−29.73	38.07	−8.87
			Amplitude excitation	0.79	0.70	0.40	0.46	0.21	0.16	0.41	0.15
		Arm	Phase excitation	−9.64	−72.07	159.50	−79.93	133.43	131.88	−98.99	92.60
			Amplitude excitation	0.97	0.66	0.46	0.01	0.64	0.40	0.26	0.36

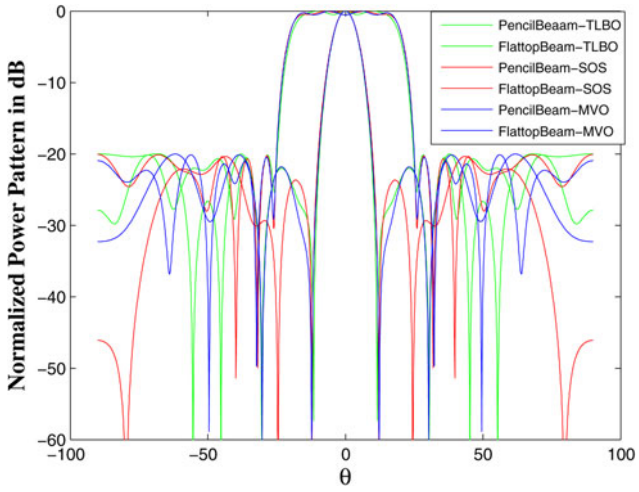


Fig. 7. Normalized power pattern in $\varphi = 0^{o}$ plane for Example 2.

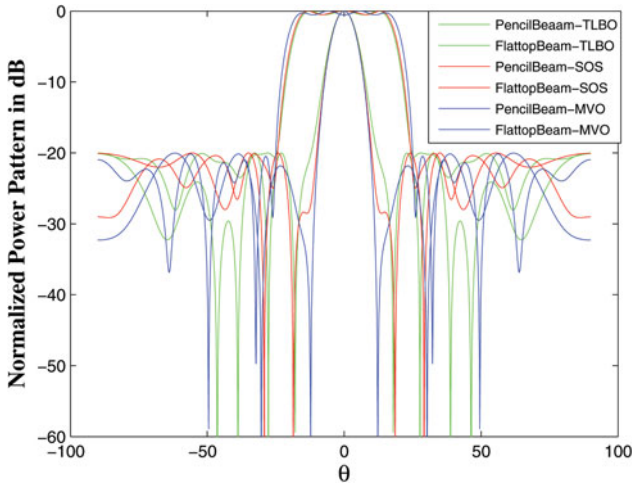


Fig. 8. Normalized power pattern in $\varphi = 90^{o}$ plane for Example 2.

the design variables are summarized in Table 1. Table 2 reports the phase excitation values corresponding to the flat-top beam using all three algorithms.

Example 2 deals with the eight-concentric hexagonal array antennas of $2N$ ($N = 6$) isotropic antennas in each of the hexagon. The antennas are placed uniformly with a spacing $d_e = 0.5\lambda$ in the first ring and the inter-ring spacing is kept at $d_h = 0.5\lambda$ between two adjacent hexagonal arrays. The desired value for SLL for the pencil and flat-top beams is kept the same as the previous example, i.e. 20 dB for both the beams. Table 3 represents the expected and calculated values of the design variables for Example 2, using all three algorithms the two φ-planes. The global best value zero indicates that the obtained values of all the design parameters are lesser than the corresponding expected values. Table 4 gives the phase distribution of the elements present at the vertices and in the arms of each hexagon. The reconfigurable power patterns using TLBO, SOS, and MVO are presented together for 0^{o} and 90^{o} φ-planes in Figs 7 and 8, respectively.

It can be noticed that the inter-element spacing in each hexagon is sufficient enough to eliminate the effect of mutual coupling. All the algorithms prove their efficiency to reach the global solution of the optimization problem. From Tables 1 and 3, it can be noticed that the SOS algorithms perform better than the other two algorithms in terms of SLL and ripple for Case 1 in both examples. Whereas in Case 2 of Examples 1 and 2, MVO obtains improved SLL and ripple values compared to TLBO and SOS optimization algorithms. In general, both examples were able to produce reconfigurable beam patterns at two principle vertical planes. Though the structure considered in Example 2 can reach the desired values of all the design parameters with a lower number of array elements and smaller structures. Also, for Example 2, all three algorithms perform almost the same and able to achieve the design objectives. These three optimization algorithms do not have any tuning parameters; hence they can support stable results with minimal complexity. Also, the proposed optimization technique can produce reconfigurable beam patterns in different azimuth planes successfully with a negligible amount of ripple in the main beam of the flat-top pattern.

Conclusion

In this paper, three well-performing meta-heuristic optimization algorithms are used to generate reconfigurable patterns in different azimuth planes by controlling the phases only and keeping the optimal amplitude distribution unmodified for generating the flat-top and pencil beam patterns. The proposed design allows us to satisfy the pattern requirements maintaining control over other design constraints. The proposed approach can essentially be utilized in high-performance radar systems and other wireless applications to produce a dynamically reconfigurable radiation pattern, uniformly at different φ-planes. The proposed work can be extended by placing nulls at desired locations, including the mutual coupling effect by considering practical antennas.

References

1. **Elliott RS** (2003) *Antenna Theory and Design*. New York: Wiley Interscience.
2. **Bucci OM, Mazzarella G and Panariello G** (1991) Reconfigurable arrays by phase-only control. *IEEE Transactions on Antennas and Propagation* **39**, 919–925.
3. **Buttazzoni G and Vescovo R** (2012) Power synthesis for reconfigurable arrays by phase-only control with simultaneous dynamic range ratio and near-field reduction. *IEEE Transactions on Antennas and Propagation* **60**, 1161–1165.
4. **Gies D and Rahmat-Samii Y** (2003) Particle swarm optimization for reconfigurable phase-differentiated array design. *Microwave and Optical Technology Letters* **38**, 168–175.
5. **Boeringer DW and Werner DH** (2004) Particle swarm optimization versus genetic algorithms for phased array synthesis. *IEEE Transactions on Antennas and Propagation* **52**, 771–779.
6. **Mahanti GK, Chakrabarty A and Das S** (2007) Phase-only and amplitude-phase synthesis of dual-pattern linear antenna arrays using floating-point genetic algorithms. *Progress in Electromagnetics Research* **68**, 247–259.
7. **Baskar S, Alphones A and Suganthan PN** (2005) Genetic-algorithm-based design of a reconfigurable antenna array with discrete phase shifters. *Microwave and Optical Technology Letters* **45**, 461–465.
8. **Li X and Yin M** (2011) Hybrid differential evolution with biogeography-based optimization for design of a reconfigurable antenna array with discrete phase shifters. *International Journal of Antennas and Propagation* **2011**, 1–12.

https://doi.org/10.1017/S1759078721000337 Published online by Cambridge University Press

9. **Yan L, Yong-Chang J, Ya-Ming Z and Yan-Yan T** (2014) Synthesis of phase-only reconfigurable linear arrays using multiobjective invasive weed optimization based on decomposition. *International Journal of Antennas and Propagation* **2011**, 1–11.
10. **Jamunaa D, Hasoon FN and Mahanti GK** (2019) Symbiotic organisms search optimisation algorithm for synthesis of phase-only reconfigurable concentric circular antenna array with uniform amplitude distribution. *International Journal of Electronics Letters* **8**.
11. **Jamunaa D, Mahanti GK and Hasoon Al Attar FN** (2019) Design of phase-only reconfigurable planar array antenna in selected phi cuts using various meta-heuristic optimization algorithms. *Sådhanå* **44**, 83.
12. **Misra B and Mahanti GK** (2020) Minimization of side lobe level of non-uniformly spaced concentric elliptical array antennas for a desired value of first null beam width in vertical and horizontal planes. *Electromagnetics* **40**, 254–261.
13. **Misra B and Mahanati GK** (2020) Side lobe level reduction of thinned concentric elliptical array antenna in vertical and horizontal plane for a desired peak directivity. *International Journal of Numerical Modelling: Electronic Networks, Devices and Fields* **34**.
14. **Castorina G, Donato LD, Morabito AF, Isernia T and Sorbello G** (2016) Analysis and design of a concrete embedded antenna for wireless monitoring applications [Antenna Applications Corner]. *IEEE Antennas and Propagation Magazine* **58**, 76–93.
15. **Rao RV and Patel V** (2013) An improved teaching-learning-based optimization algorithm for solving unconstrained optimization problems. *Scientia Iranica* **20**, 710–720.
16. **Cheng MY and Prayogo D** (2014) Symbiotic organisms search: a new metaheuristic optimization algorithm. *Computers and Structures* **139**, 98–112.
17. **Mirjalili S, Mirjalili SM and Hatamlou A** (2016) Multi-verse optimizer: a nature-inspired algorithm for global optimization. *Neural Computing and Applications* **27**, 495–513.
18. **Gozasht F, Dadashzadeh GR and Nikmehr S** (2007) A comprehensive performance study of circular and hexagonal array geometries in the LMS algorithm for smart antenna applications. *Progress in Electromagnetics Research* **68**, 281–296.
19. **Kretly LC, Cerqueira Jr AS and Tavora AAS** (2002) A hexagonal adaptive antenna array concept for wireless communication applications, The 13th IEEE International Symposium on Personal, Indoor and Mobile Radio Communications, **1**, 247–249.
20. **Mahmoud KR, El-Adway M, Ibrahem SMM, Basnel R, Mahmoud R and Zainud-Deen SH** (2007) A comparison between circular and hexagonal array geometries for smart antenna systems using particle swarm algorithm. *Progress in Electromagnetics Research [PIER]* **72**, 75–90.
21. **Bera R, Lanjewar R, Mandal D, Kar R and Ghoshal SP** (2015) Comparative Study of Circular and Hexagonal Antenna Array Synthesis using Improved Particle Swarm Optimization, International Conference on Advanced Computing Technologies and Applications (ICACTA-2015), Procedia Computer Science **45**, 651–660.



Bitan Misra received B.Tech and M.Tech dual degree in Electronics and Communication Engineering from the KIIT University, Bhubaneswar, India in 2018. Presently, she is pursuing her Ph.D. in the Department of Electronics and Communication Engineering at the National Institute of Technology, Durgapur, India. Her main research interests include optimization techniques, array antenna synthesis, evolutionary algorithms, and soft-computing techniques.



G.K. Mahanti was born in the year 1967 in West Bengal, India. He obtained his B.E. in Electronics & Communication Engineering from the NIT, Durgapur, India, M.E. in Electronics System and Communication from the NIT, Rourkela, India and Ph.D. from the Department of Electronics and Electrical Communication Engineering, IIT, Kharagpur, India. He has more than 28 years of teaching and research experience. Presently, he is working as a Professor of the Department of Electronics and Communication Engineering, National Institute of Technology, Durgapur, India. He is a senior member of IEEE, USA. He has published approximately 100 papers in journals and in national and international conferences. He was the reviewer of many international journals like Electronics Letter, IEEE Antennas and Wireless Propagation Letter, IEEE Transaction on Antenna and Propagation, Progress in Electromagnetics Research, IET Microwave, Antenna and Propagation and many conferences. His biography is listed in Marqui's Who is Who in the world. His research area is array antenna synthesis, meta-heuristic optimization algorithms & electromagnetics.

https://doi.org/10.1017/S1759078721000337 Published online by Cambridge University Press